

# USIS-PGM: Photometric Gaussian Mixtures for Underwater Salient Instance Segmentation

1<sup>st</sup> Lin Hong

*Department of Electronic and Computer Engineering  
The Hong Kong University of Science and Technology  
Hong Kong, China  
eelinhong@ust.hk*

2<sup>nd</sup> Xiangtong Yao

*Department of Informatics  
Technical University of Munich  
Munich, Germany  
xiangtong.yao@tum.de*

3<sup>rd</sup> Mürüvvet Bozkurt

*Department of Informatics  
Technical University of Munich  
Munich, Germany  
mbozkurt76@gmail.com*

4<sup>th</sup> Xin Wang

*School of Robotics and Advanced Manufacture  
Harbin Institute of Technology (Shenzhen)  
Shenzhen, China  
wangxinsz@hit.edu.cn*

5<sup>th</sup> Fumin Zhang

*Department of Electronic and Computer Engineering  
The Hong Kong University of Science and Technology  
Hong Kong, China  
eefumin@ust.hk*

**Abstract**—Underwater salient instance segmentation (USIS) is crucial for marine robotic systems, as it enables both underwater salient object detection and instance-level mask prediction for visual scene understanding. Compared with its terrestrial counterpart, USIS is more challenging due to the underwater image degradation. To address this issue, this paper proposes USIS-PGM, a single-stage framework for USIS. Specifically, the encoder enhances boundary cues through a frequency-aware module and performs content-adaptive feature reweighting via a dynamic weighting module. The decoder incorporates a Transformer-based instance activation module to better distinguish salient instances. In addition, USIS-PGM employs multi-scale Gaussian heatmaps generated from ground-truth masks through Photometric Gaussian Mixture (PGM) to supervise intermediate decoder features, thereby improving salient instance localization and producing more structurally coherent mask predictions. Experimental results demonstrate the superiority and practical applicability of the proposed USIS-PGM model.

## I. INTRODUCTION

Visual perception plays a critical role in underwater robotic systems for a wide range of applications, including marine exploration [1], biodiversity monitoring [2], and underwater infrastructure inspection [3]. In these scenarios, underwater robots are often required not only to detect visually important regions, but also to distinguish individual object instances for downstream decision-making and interaction. Underwater Salient Instance Segmentation (USIS) [4], [5], which jointly addresses *where to look* (saliency prediction) and *what is there* (instance segmentation) in underwater scenes, has therefore emerged as a fundamental task for underwater visual scene understanding. By simultaneously performing underwater salient object detection [6] and predicting their instance-level masks, USIS is particularly valuable for visual perception of underwater robots in complex environments.

Despite its importance, USIS remains highly challenging. In contrast to terrestrial scenes, underwater imagery is severely affected by absorption and scattering of light, wavelength-dependent attenuation, and non-uniform illumination. These factors often lead to low contrast, color distortion, and blurred boundaries, which significantly degrade the discriminability of visual features [7]. Moreover, underwater environments exhibit dynamic backgrounds, frequent scale variation, and diversity across species and man-made objects. Such characteristics make it difficult to accurately localize underwater salient objects and predict precise masks from images.

In terrestrial environments, salient instance segmentation has been widely studied and has achieved notable progress [8]–[10]. However, these methods cannot be directly transferred to underwater scenes in an off-the-shelf manner. The domain gap between terrestrial and underwater imagery is substantial, not only because of the distinct imaging physics, but also due to differences in object categories, visual appearance, and scene composition. In particular, object categories in underwater imagery often follow long-tailed distributions, with some classes appearing frequently while many others are sparsely represented. This further limits the generalization ability of models originally developed for terrestrial environments.

To address these challenges, existing research on USIS has mainly progressed along two complementary directions. The first direction focuses on constructing large-scale datasets to support model development and evaluation. Representative examples include USIS10K [4] and USIS16K [5]. Specifically, USIS10K contains 10,632 underwater images with pixel-level annotations across 7 categories collected from diverse underwater scenes, while USIS16K includes 16,151 underwater images with multi-level annotations and covers 158 object categories. These datasets have significantly advanced the study of USIS by providing stronger benchmark support.

The second direction aims to design more robust models that explicitly account for underwater image degradation and the

\*The work described in this paper was partially supported by grants AoE/E-601/24-N, 16203223, C6029-23G, and C6078-25G from the Research Grants Council of the Hong Kong Special Administrative Region, China.

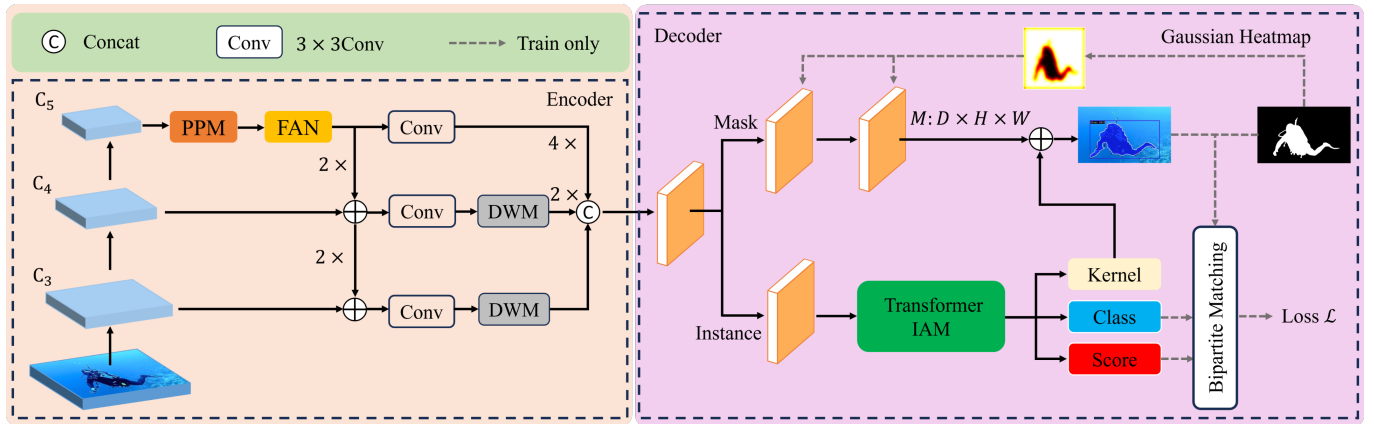


Fig. 1. Overall framework of the proposed USIS-PGM model, consisting of an encoder, a decoder, and the PGM-based multi-scale supervision strategy. The encoder integrates FAN and DWM to enhance boundary-aware representation and content-adaptive feature reweighting, while the decoder employs a Transformer-based IAM for accurate salient instance localization and mask prediction.

cross-domain gap between terrestrial and underwater scenes. For example, [4] provided an underwater-specific baseline for USIS10K by adapting the Segment Anything Model [11], termed USIS-SAM. It introduces an underwater-aware vision transformer encoder to incorporate underwater-domain visual prompts into the segmentation network. Although such efforts demonstrate the promise of underwater-oriented architectural adaptation, existing methods still face notable limitations. In particular, under severe degradation, intermediate features in the network can be easily distracted by low-level photometric corruption and background noise, which often leads to inaccurate salient instance localization, fragmented masks, and poor separation between adjacent instances. This suggests that, beyond simply strengthening backbone feature extraction, it is also important to impose more effective structural guidance on intermediate representations during decoding.

In this work, we argue that *Photometric Gaussian Mixture* (PGM) [12] offers a promising solution to this problem. The central intuition is that Gaussian-distributed photometric priors provide compact yet informative guidance for modeling the spatial distribution, extent, and structural organization of salient instances. Compared with direct binary supervision, PGM-based supervision yields smoother and more ambiguity-tolerant training signals, which are particularly suitable for underwater scenes where object boundaries are often blurred and appearance cues are unstable. By incorporating multi-scale Gaussian heatmap guidance derived from ground-truth masks, the network is encouraged to learn more discriminative and spatially coherent intermediate representations, thereby improving both salient instance localization and mask prediction.

Motivated by this observation, this paper proposes **USIS-PGM**, a dedicated single-stage architecture for USIS that explicitly incorporates *Photometric Gaussian Mixture* (PGM)-based supervision. Specifically, the encoder enhances boundary-aware representations through a frequency-aware module and performs content-adaptive feature reweighting via a dynamic weighting module. On the decoder side, a

Transformer-based instance activation module is introduced to better distinguish salient instances and improve instance separation. Furthermore, intermediate decoder features are explicitly supervised by multi-scale Gaussian heatmaps generated from ground-truth masks. Extensive experiments on the USIS16K dataset demonstrate that the proposed USIS-PGM model outperforms existing methods. The results further show that incorporating PGM-based supervision not only improves salient object localization, but also enhances mask completeness and structural consistency under underwater conditions. The contributions of this paper are summarized as follows:

- We propose **USIS-PGM**, a single-stage framework for USIS that explicitly introduces PGM generate multi-scale Gaussian heatmaps, which are used to guide intermediate decoder features and promote more effective learning of salient instance localization and mask prediction.
- The proposed USIS-PGM integrates frequency-aware boundary enhancement, dynamic feature reweighting, and Transformer-based instance activation into a unified architecture to better address underwater image degradation and improve salient instance segmentation.
- Extensive experiments on the USIS16K dataset demonstrate the effectiveness and superiority of the proposed USIS-PGM model over benchmark methods.

## II. USIS-PGM MODEL

The overall architecture of the proposed USIS-PGM model is illustrated in Fig. 1. USIS-PGM is designed as a single-stage framework consisting of three main components: an encoder, a decoder, and a PGM-guided multi-scale supervision.

### A. Encoder Design

Underwater imagery often suffers from low contrast and blurred boundaries. These factors make it difficult for standard feature extractors to preserve both semantic consistency and local structural details. To address this issue, the encoder incorporates two modules, i.e., frequency adjust network (FAN), and dynamic weight module (DWM).

**FAN** is designed to enhance fine edges and contour details by reweighting the frequency content of feature maps. Its main motivation is that low-frequency components primarily describe global intensity and coarse structural information, whereas high-frequency components contain boundary, edge, and texture cues that are especially important for accurate object delineation. This distinction is particularly relevant in underwater scenes, where image degradation often weakens boundary visibility and makes salient instances difficult to separate from the background. Based on this observation, FAN first transforms the input feature map into the frequency domain and emphasizes the high-frequency responses that are more closely related to edges and local structural variations. The selected frequency components are then converted back into the spatial domain to produce a gain map, which highlights regions with strong boundary and texture information. Finally, this gain map is applied to the original feature map in a residual manner, so that informative edge-sensitive responses are enhanced while the original low-frequency content and overall semantic structure are preserved.

**DWM** is designed to improve feature adaptivity by learning input-dependent weights to modulate feature responses. Specifically, the input feature map is first compressed through two consecutive convolutional layers to obtain a compact representation with reduced channel dimensionality. The compressed feature is then flattened, and dynamic modulation weights are generated from the feature content itself, enabling content-aware reweighting of individual feature elements. After modulation, the feature is reshaped back into the spatial domain and projected to the original channel dimension. In our implementation, DWM is applied to the higher-level encoder branches  $C_4$  and  $C_5$ . To reduce computational cost, these branches are first resized to a fixed spatial resolution, processed by DWM, and then upsampled back to their original size. Through this content-adaptive reweighting mechanism, DWM helps the network emphasize salient-instance-related information while suppressing noisy and irrelevant responses.

### B. Decoder with Instance Activation Module

The decoder is designed to progressively reconstruct dense masks for USIS. One of the central challenges in USIS is to accurately separate nearby or partially overlapping salient objects, particularly when their appearance is degraded and their boundaries are ambiguous. To address this challenge, we incorporate a Transformer-based Instance Activation Module (IAM) into the decoder. The key idea of IAM is to enhance instance-aware feature interaction and activation [13]. Unlike conventional convolution-based decoding, the Transformer [14] is capable of capturing long-range dependencies and modeling global relationships across spatial regions. This property is especially beneficial in underwater scenes, where local visual evidence alone is often insufficient to distinguish adjacent instances under blur, occlusion, or low contrast. By exploiting self-attention, IAM dynamically aggregates contextual cues from different locations and highlights features that are informative for salient instance separation. Specifically,

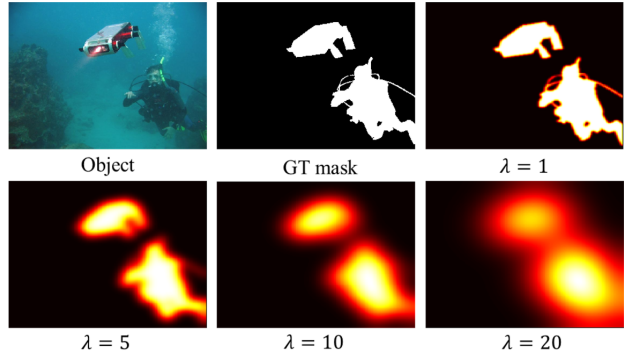


Fig. 2. Visualization of Gaussian heatmaps generated from ground-truth mask based on  $G(I; \lambda)$ , where  $\lambda = \{1, 5, 10, 20\}$ .

IAM takes decoder features as input and refines them through instance-aware attention modeling. This process promotes better disentanglement of features associated with different salient regions while suppressing ambiguous background responses.

### C. PGM-based Multi-scale Supervision

To improve intermediate decoder representation learning, we introduce a multi-scale supervision strategy based on PGM. The underlying motivation is that binary mask supervision imposed only at the final output layer may be insufficient to guide intermediate features toward accurate salient-instance localization and structural modeling, especially in underwater images with blurred boundaries and unstable visual appearance. In contrast, Gaussian heatmaps generated from ground-truth masks provide smoother and more spatially structured supervisory signals, making them better suited to progressively guiding feature learning across different decoding stages.

A two-dimensional Gaussian function provides a natural way to model spatial influence that gradually decays with distance from a center location. Let  $x \in \mathbb{R}$  and  $y \in \mathbb{R}$  denote two spatial variables, and let  $\mathbf{x} = (x, y)^\top$ . The two-dimensional Gaussian function is defined as

$$f(x, y) = A \exp\left(-\frac{(x - x_0)^2}{2\sigma_x^2} - \frac{(y - y_0)^2}{2\sigma_y^2}\right), \quad (1)$$

where  $A$  denotes the amplitude,  $(x_0, y_0)$  represents the Gaussian center, and  $\sigma_x$  and  $\sigma_y$  control the spread along the horizontal and vertical directions, respectively.

**Photometric Gaussian Mixture (PGM).** Let an image be defined on the pixel grid  $\mathcal{U}$ , where each pixel coordinate is denoted by  $\mathbf{u} = (u, v)^\top$  and the corresponding luminance value is  $I(\mathbf{u})$ . Following [12], PGM is formulated as

$$G(I; \lambda)(\mathbf{x}) = \sum_{\mathbf{u} \in \mathcal{U}} I(\mathbf{u}) \exp\left(-\frac{\|\mathbf{x} - \mathbf{u}\|^2}{2\lambda^2}\right), \quad (2)$$

where  $\lambda$  is a shared isotropic extension parameter that controls the spatial spread of each Gaussian component.

In our setting, the Gaussian center is aligned with the pixel position, i.e.,  $(x_0, y_0) = \mathbf{u}$ , the amplitude is defined by the pixel intensity, i.e.,  $A = I(\mathbf{u})$ , and isotropic extension is adopted by setting  $\sigma_x = \sigma_y = \lambda$ . In this way, each pixel

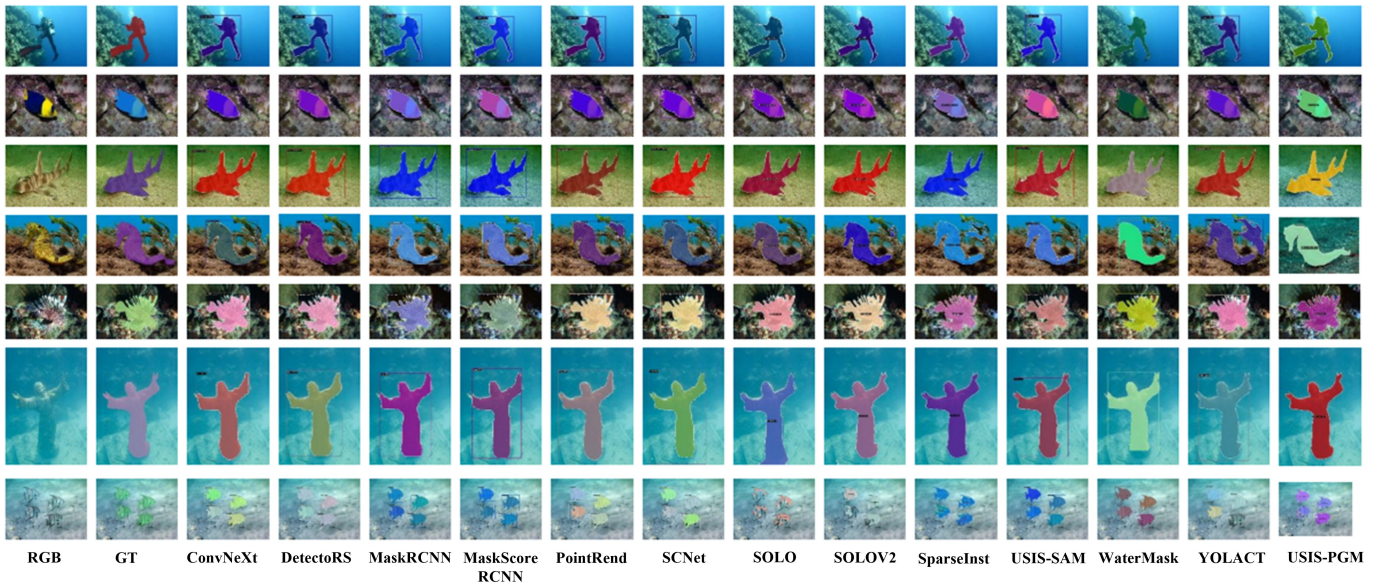


Fig. 3. Qualitative evaluation of the proposed USIS-PGM model with 12 benchmark methods on the USIS16K dataset.

contributes a local Gaussian component, and the final heatmap is obtained by aggregating all Gaussian responses over the mask region. As illustrated in Fig. 2, different values of  $\lambda$  produce Gaussian heatmaps at different spatial scales.

#### D. Training Objective with Multi-scale Supervision

We use the generated multi-scale Gaussian heatmaps to supervise intermediate decoder features. Compared with hard binary labels, these heatmaps encode not only target presence but also the relative spatial importance of pixels around salient instances. This provides richer structural guidance and enables the network to progressively learn the spatial extent, central tendency, and structural distribution of foreground objects. Accordingly, the Gaussian heatmap loss is introduced as an auxiliary term in the overall training objective. By complementing the classification and mask-based losses, it further improves the quality of intermediate feature learning.

Since USIS requires the model to simultaneously perform object-level recognition and pixel-level segmentation, multiple loss terms are jointly optimized during training. The overall training objective is formulated as

$$\mathcal{L} = \lambda_{\text{cls}}\mathcal{L}_{\text{cls}} + \lambda_{\text{obj}}\mathcal{L}_{\text{obj}} + \lambda_{\text{mask}}\mathcal{L}_{\text{mask}} + \lambda_{\text{dice}}\mathcal{L}_{\text{dice}} + \lambda_{\text{gh}}\mathcal{L}_{\text{gh}}. \quad (3)$$

Here,  $\mathcal{L}_{\text{cls}}$  supervises instance category prediction,  $\mathcal{L}_{\text{obj}}$  supervises object-level detection,  $\mathcal{L}_{\text{mask}}$  constrains the pixel-wise quality of predicted masks,  $\mathcal{L}_{\text{dice}}$  improves mask overlap and alleviates foreground-background imbalance, and  $\mathcal{L}_{\text{gh}}$  serves as an auxiliary term for guiding intermediate representations with multi-scale Gaussian heatmaps. The weighting coefficients  $\lambda_{\text{cls}}$ ,  $\lambda_{\text{obj}}$ ,  $\lambda_{\text{mask}}$ ,  $\lambda_{\text{dice}}$ , and  $\lambda_{\text{gh}}$  control the relative contributions of the corresponding loss terms.

### III. IMPLEMENTATION DETAILS

The proposed USIS-PGM model is implemented in PyTorch. All experiments are conducted on an Ubuntu 20.04 platform with an NVIDIA GeForce RTX 3090 GPU and CUDA support. We use the USIS16K dataset for training and evaluation. In this dataset, the underwater images and their corresponding depth maps are uniformly resized to  $640 \times 480 \times 3$ . To ensure effective model training, the batch size is set to 4, and the model is trained for a total of 500,000 iterations with an initial learning rate of  $5 \times 10^{-5}$  and a weight decay of 0.0001. The weights for the classification loss, mask loss, Dice loss, and Gaussian heatmap loss are set to  $\lambda_{\text{cls}} = \lambda_{\text{obj}} = \lambda_{\text{mask}} = \lambda_{\text{dice}} = \lambda_{\text{gh}} = 0.2$ .

### IV. EVALUATION AND ANALYSIS

#### A. Evaluation protocol

The proposed USIS-PGM model is comprehensively evaluated on the USIS16K dataset against 12 benchmark methods, including Mask R-CNN [15], Mask Scoring R-CNN [16], YOLACT [17], SOLO [18], SOLOV2 [19], PointRend [20], DetectoRS [21], SCNet [22], SparseInst [23], ConvNeXt [24], WaterMask [25], and USIS-SAM [4]. For fairness, all competing methods are evaluated under the same dataset protocol and standard evaluation settings. Furthermore, ablation studies are conducted to verify the effectiveness of the proposed PGM-based multi-scale supervision strategy.

#### B. Qualitative Evaluation

To provide a more intuitive comparison, Fig. 3 presents representative qualitative results of USIS-PGM and 12 benchmark methods on underwater images from the USIS16K dataset. The visual comparisons show that USIS-PGM generates more complete and accurate salient instance masks, especially in

TABLE I  
QUANTITATIVE EVALUATION RESULTS OF THE USIS-PGM MODEL.

Methods	$mAP(\uparrow)$	$AP_{50}(\uparrow)$	$AP_{75}(\uparrow)$	$AP_S(\uparrow)$	$AP_M(\uparrow)$	$AP_L(\uparrow)$
Mask R-CNN [15]	.736	.900	.817	.400	.604	.745
Mask Scoring R-CNN [16]	.716	.885	.798	.450	.515	.726
YOLOACT [17]	.754	.904	.826	.450	.545	.760
SOLO [18]	.595	.763	.659	.119	.327	.606
SOLOV2 [19]	.717	.859	.771	.450	.482	.726
PointRend [20]	.763	.894	.827	.500	.659	.774
DetectorRS [21]	.732	.938	.872	.433	.664	.788
SCNet [22]	.752	.910	.822	.475	.630	.759
SparseInst [23]	.730	.850	.769	.450	.449	.740
ConvNeXt [24]	.785	.953	.879	.551	.688	.792
Watermask [25]	.727	.868	.793	.417	.570	.736
USIS-SAM [4]	.810	.908	.871	.450	.643	.818
USIS-PGM (ours)	<b>.816</b>	.912	<b>.882</b>	<b>.568</b>	<b>.670</b>	.814

challenging scenarios involving low visibility, complex backgrounds, and ambiguous object boundaries.

In particular, the masks predicted by USIS-PGM exhibit more precise boundary delineation, fewer missing regions, and clearer separation between adjacent instances. These advantages are especially evident in scenes containing multiple salient objects or thin structures, where benchmark methods often suffer from incomplete masks, false positives, or confusion between neighboring instances. As a result, USIS-PGM produces masks that are not only more accurate but also more spatially coherent. These qualitative observations confirm the effectiveness and superiority of the proposed USIS-PGM.

### C. Quantitative Evaluation

To quantitatively evaluate the performance of USIS-PGM, we compare it with 12 benchmark methods on the USIS16K dataset. As shown in Table I, USIS-PGM achieves the best overall mAP of 0.816, outperforming all competing methods, including the underwater-specific model USIS-SAM, which attains an mAP of 0.810. Moreover, USIS-PGM obtains the highest  $AP_{75}$  of 0.882 and the best  $AP_S$  of 0.568, indicating that the proposed model is particularly effective at producing accurate masks and handling small salient instances under challenging underwater conditions. USIS-PGM also achieves a competitive  $AP_M$  of 0.670 and an  $AP_L$  of 0.814, demonstrating robust performance across different object scales. Although its  $AP_{50}$  is not the highest among all compared methods, its superior results on the more stringent metrics mAP and  $AP_{75}$  suggest better overall localization quality and mask accuracy.

Fig. 4 presents the precision–recall (PR) curves of 12 benchmark methods and the proposed USIS-PGM model on four randomly selected object categories from the USIS16K dataset. It can be observed that USIS-PGM outperforms most competing methods on three categories, namely Diver, Swimmer, and Plastic Cup, demonstrating its strong category-level detection and segmentation capability. Although there is still room for improvement in certain categories, the overall PR-curve performance further confirms the effectiveness of the proposed model. In addition, USIS-SAM and WaterMask, as underwater-specific methods, outperform most benchmark methods originally developed for terrestrial environments, highlighting the importance of domain-specific design for underwater visual perception.

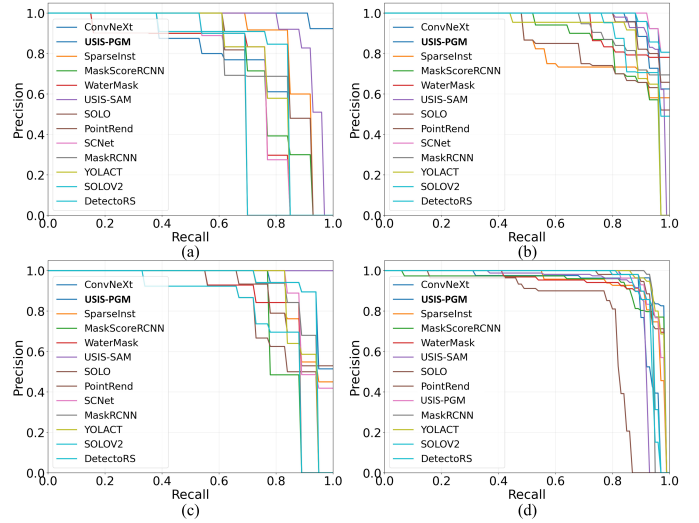


Fig. 4. PR curve performance of the proposed USIS-PGM model and 12 benchmark methods on four representative object categories, i.e., (a) Diver, (b) Swimmer, (c) Plastic cup, and (d) Sea chest grating.

TABLE II  
ABLATION STUDY OF THE PGM-BASED MULTI-SCALE SUPERVISION IN THE USIS-PGM MODEL.

Methods	$mAP(\uparrow)$	$AP_{50}(\uparrow)$	$AP_{75}(\uparrow)$	$AP_S(\uparrow)$	$AP_M(\uparrow)$	$AP_L(\uparrow)$
USIS-PGM (-PGM)	.798	.889	.859	.540	.549	.809
USIS-PGM (ours)	<b>.816</b>	<b>.912</b>	<b>.882</b>	<b>.568</b>	<b>.670</b>	<b>.814</b>

Overall, the qualitative and quantitative results consistently demonstrate the effectiveness and superiority of USIS-PGM.

### D. Ablation Study of PGM-based Multi-scale Supervision

To further validate the effectiveness of the proposed PGM-based multi-scale supervision, we report the ablation results in Table II. Specifically, the full USIS-PGM model is compared with a variant without PGM-based multi-scale supervision, i.e., (USIS-PGM(-PGM)), in order to isolate the contribution of the proposed supervision strategy. As shown in Table II, introducing PGM brings consistent improvements across all evaluation metrics. In particular, mAP increases from 0.798 to 0.816, while  $AP_{50}$  and  $AP_{75}$  improve from 0.889 to 0.912 and from 0.859 to 0.882, respectively. In terms of object scale,  $AP_S$ ,  $AP_M$ , and  $AP_L$  increase from 0.540 to 0.568, from 0.549 to 0.670, and from 0.809 to 0.814, respectively. Notably, the largest gain is observed on medium-sized objects, indicating that the proposed PGM-based multi-scale supervision is particularly effective in improving instance localization and structural modeling at this scale.

### E. Applications in Underwater Object Reconstruction

To further demonstrate the practical applicability of USIS-PGM, we integrate the model into an underwater object reconstruction pipeline. Specifically, USIS-PGM is first employed to predict masks for underwater salient instances, such as sacrificial anodes and sea snails, from raw underwater images. The resulting segmentation masks are then used as foreground

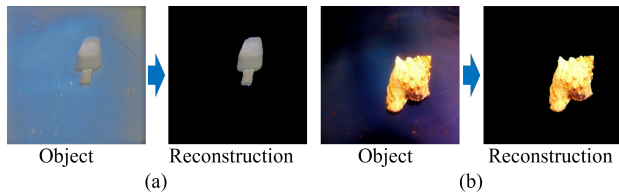


Fig. 5. 3D reconstruction results of underwater objects, including (a) sacrificial anodes and (b) sea snails, obtained using USIS-PGM and COLMAP [26].

priors in COLMAP [26] for reconstructing the 3D geometry of the target objects. As shown in Fig. 5, accurate salient instance segmentation effectively reduces background interference and improves the structural completeness of the reconstructed underwater objects.

## V. CONCLUSION

This paper presented USIS-PGM model for underwater salient instance segmentation. To address the challenges arising from underwater image degradation, the proposed model integrates multi-scale contextual aggregation, frequency-aware boundary enhancement, dynamic feature reweighting, and a Transformer-based instance activation module into a unified single-stage architecture. Furthermore, a multi-scale Gaussian heatmap supervision strategy based on Photometric Gaussian Mixture was introduced to guide intermediate decoder features, thereby promoting more discriminative and spatially coherent learning of salient instance localization and mask structure. Extensive experiments on benchmark datasets demonstrated that USIS-PGM outperforms existing benchmark methods. Its practical applicability was further demonstrated through underwater object reconstruction experiments. In future work, we will investigate more efficient architectures for underwater robotic visual perception.

## REFERENCES

- [1] D. Mallet and D. Pelletier, "Underwater video techniques for observing coastal marine biodiversity: a review of sixty years of publications (1952–2012)," *Fisheries Research*, vol. 154, pp. 44–62, 2014.
- [2] X.-R. Huang and L.-B. Chen, "An underwater explorer remotely operated vehicle: Unraveling the secrets of the ocean," *IEEE potentials*, vol. 42, no. 3, pp. 31–36, 2023.
- [3] L. Hong, X. Wang, D.-S. Zhang, M. Zhao, and H. Xu, "Vision-based underwater inspection with portable autonomous underwater vehicle: Development, control, and evaluation," *IEEE Transactions on Intelligent Vehicles*, vol. 9, no. 1, pp. 2197–2209, 2023.
- [4] S. Lian, Z. Zhang, H. Li, W. Li, L. T. Yang, S. Kwong, and R. Cong, "Diving into underwater: Segment anything model guided underwater salient instance segmentation and a large-scale dataset," in *Proceedings of the 41st International Conference on Machine Learning*, pp. 29545–29559, 2024.
- [5] L. Hong, X. Wang, Y. Li, and X. Wang, "Usis16k: High-quality dataset for underwater salient instance segmentation," *arXiv preprint arXiv:2506.19472*, 2025.
- [6] L. Hong, X. Wang, G. Zhang, and M. Zhao, "Usod10k: a new benchmark dataset for underwater salient object detection," *IEEE transactions on image processing*, vol. 34, pp. 1602–1615, 2023.
- [7] L. Hong, X. Wang, Z. Xiao, G. Zhang, and J. Liu, "Wsuie: Weakly supervised underwater image enhancement for improved visual perception," *IEEE Robotics and Automation Letters*, vol. 6, no. 4, pp. 8237–8244, 2021.

- [8] R. Fan, M.-M. Cheng, Q. Hou, T.-J. Mu, J. Wang, and S.-M. Hu, "S4net: Single stage salient-instance segmentation," in *Proceedings of the IEEE/CVF conference on computer vision and pattern recognition*, pp. 6103–6112, 2019.
- [9] Y.-H. Wu, Y. Liu, L. Zhang, W. Gao, and M.-M. Cheng, "Regularized densely-connected pyramid network for salient instance segmentation," *IEEE Transactions on Image Processing*, vol. 30, pp. 3897–3907, 2021.
- [10] J. Pei, T. Jiang, H. Tang, N. Liu, Y. Jin, D.-P. Fan, and P.-A. Heng, "Calibnet: Dual-branch cross-modal calibration for rgb-d salient instance segmentation," *IEEE Transactions on Image Processing*, vol. 33, pp. 4348–4362, 2024.
- [11] A. Kirillov, E. Mintun, N. Ravi, H. Mao, C. Rolland, L. Gustafson, T. Xiao, S. Whitehead, A. C. Berg, W.-Y. Lo, *et al.*, "Segment anything," in *Proceedings of the IEEE/CVF international conference on computer vision*, pp. 4015–4026, 2023.
- [12] N. Crombez, E. M. Mouaddib, G. Caron, and F. Chaumette, "Visual servoing with photometric gaussian mixtures as dense features," *IEEE Transactions on Robotics*, vol. 35, no. 1, pp. 49–63, 2018.
- [13] T. Cheng, X. Wang, S. Chen, W. Zhang, Q. Zhang, C. Huang, Z. Zhang, and W. Liu, "Sparse instance activation for real-time instance segmentation," in *Proceedings of the IEEE/CVF conference on computer vision and pattern recognition*, pp. 4433–4442, 2022.
- [14] A. Vaswani, N. Shazeer, N. Parmar, J. Uszkoreit, L. Jones, A. N. Gomez, Ł. Kaiser, and I. Polosukhin, "Attention is all you need," *Advances in neural information processing systems*, vol. 30, 2017.
- [15] K. He, G. Gkioxari, P. Dollár, and R. Girshick, "Mask r-cnn," in *Proceedings of the IEEE international conference on computer vision*, pp. 2961–2969, 2017.
- [16] Z. Huang, L. Huang, Y. Gong, C. Huang, and X. Wang, "Mask scoring r-cnn," in *Proceedings of the IEEE/CVF conference on computer vision and pattern recognition*, pp. 6409–6418, 2019.
- [17] D. Bolya, C. Zhou, F. Xiao, and Y. J. Lee, "Yolact: Real-time instance segmentation," in *Proceedings of the IEEE/CVF international conference on computer vision*, pp. 9157–9166, 2019.
- [18] X. Wang, T. Kong, C. Shen, Y. Jiang, and L. Li, "Solo: Segmenting objects by locations," in *Computer Vision—ECCV 2020: 16th European Conference, Glasgow, UK, August 23–28, 2020, Proceedings, Part XVIII 16*, pp. 649–665, Springer, 2020.
- [19] X. Wang, R. Zhang, T. Kong, L. Li, and C. Shen, "Solov2: Dynamic and fast instance segmentation," *Advances in Neural information processing systems*, vol. 33, pp. 17721–17732, 2020.
- [20] A. Kirillov, Y. Wu, K. He, and R. Girshick, "Pointrend: Image segmentation as rendering," in *Proceedings of the IEEE/CVF conference on computer vision and pattern recognition*, pp. 9799–9808, 2020.
- [21] S. Qiao, L.-C. Chen, and A. Yuille, "Detectors: Detecting objects with recursive feature pyramid and switchable atrous convolution," in *Proceedings of the IEEE/CVF conference on computer vision and pattern recognition*, pp. 10213–10224, 2021.
- [22] T. Vu, H. Kang, and C. D. Yoo, "Scnet: Training inference sample consistency for instance segmentation," in *Proceedings of the AAAI Conference on Artificial Intelligence*, vol. 35, pp. 2701–2709, 2021.
- [23] T. Cheng, X. Wang, S. Chen, W. Zhang, Q. Zhang, C. Huang, Z. Zhang, and W. Liu, "Sparse instance activation for real-time instance segmentation," in *Proc. IEEE Conf. Computer Vision and Pattern Recognition (CVPR)*, 2022.
- [24] Z. Liu, H. Mao, C.-Y. Wu, C. Feichtenhofer, T. Darrell, and S. Xie, "A convnet for the 2020s," in *Proceedings of the IEEE/CVF conference on computer vision and pattern recognition*, pp. 11976–11986, 2022.
- [25] S. Lian, H. Li, R. Cong, S. Li, W. Zhang, and S. Kwong, "Watermask: Instance segmentation for underwater imagery," in *Proceedings of the IEEE/CVF International Conference on Computer Vision*, pp. 1305–1315, 2023.
- [26] J. L. Schonberger and J.-M. Frahm, "Structure-from-motion revisited," in *Proceedings of the IEEE conference on computer vision and pattern recognition*, pp. 4104–4113, 2016.